Order−Disorder Transition Induced by the Hydroxylation of Homogeneous Polystyrene-*block*-polyisoprene Copolymer

Kyung Min Lee and Chang Dae Han*

Department of Polymer Engineering, The University of Akron, Akron, Ohio 44325

Received June 25, 2001

ABSTRACT: Three homogeneous polystyrene-*block*-polyisoprene (SI diblock) copolymers with varying block length ratios (SI-10/6, SI-5/6, and SI-14/3) were synthesized via anionic polymerization in tetrahydrofuran as solvent, giving rise to the microstructures of polyisoprene (PI) block of 34% 1,2-addition, 59% 3,4-addition, and 7% 1,4-addition. Subsequently, the SI diblock copolymers were subjected to hydroboration/oxidation reactions to yield hydroxylated SI diblock (SI-OH) copolymers (SI-10/6-OH, SI-5/6-OH, and SI-14/3-OH). After the hydroxylation, the molecular weight of SI-OH is increased by 3−9%, depending on the block length ratio of the corresponding SI diblock copolymer. Infrared (IR) spectroscopy has shown that the SI-OH diblock copolymers form hydrogen bonding at room temperature. Transmission electron microscopy has revealed that at room temperature SI-10/6-OH and SI-5/6-OH have lamellar microdomains while SI-14/3-OH has hexagonally packed cylindrical microdomains. Oscillatory shear rheometry has indicated that the order−disorder transition (ODT) temperature (T_{ODT}) of SI-14/3-OH is about 195 °C, while the T_{ODT} of SI-5/6-OH and SI-10/6-OH is much higher than 220 °C, the highest experimental temperature employed. In-situ IR spectroscopy has indicated that the strength of hydrogen bonding in SI-OH diblock copolymer decreases with increasing temperature. Specifically, it has been found that the hydrogen bonding in SI-14/3-OH virtually disappears as the temperature is increased to 200 °C, which coincides with the value of T_{ODT} determined from oscillatory shear rheometry. On the other hand, in-situ IR spectroscopy has indicated that hydrogen bonding in SI-5/6-OH and SI-10/6-OH still persists as the temperature is increased to 220 °C, the highest experimental temperature employed. The above observations lead us to conclude that the ODT induced by the hydroxylation of homogeneous SI diblock copolymers is associated with the presence of hydrogen bonding in the SI-OH diblock copolymers. Segmental interactions between PS and hydroxylated polyisoprene (PI-OH) were investigated via cloud point measurement, for which low-molecular-weight polystyrene (PS) and polyisoprene (PI) were synthesized, and the PI was hydroxylated to yield PI-OH with varying degrees of hydroxylation. It has been found that the extent of repulsive segmental interactions between PS and PI-OH increases as the degree of hydroxylation of PI increases.

Introduction

During the past two decades, the order−disorder transition (ODT) in block copolymer has extensively been investigated. There are too many papers to cite them all here; thus, the readers are referred to recent reviewer papers.[1,2] According to the currently held mean-field theories,[3−6] ODT in monodisperse, conformationally symmetric block copolymer is determined by the segregation power χN and block composition f, in which χ denotes the segmental interaction parameter of the constituent blocks and N denotes the degree of polymerization. Much of the past research activities focused on the effects of χ, N, and/or f on the ODT in block copolymers. Note that χ is inversely proportional to the absolute temperature.

Note that χ reflects the chemical structures of a polymer pair. Thus, understandably, χ varies with the chemical structures of the constituent blocks in block copolymer. Today it is well established that χ becomes positive and moves farther away from zero when the extent of repulsive segmental interactions in a polymer pair is increased, while χ is negative when a polymer pair have attractive segmental interactions. Values of χ between two components can be varied by modifying the chemical structure(s) of one or both components in a polymer blend or block copolymer. Hydrogenation of polybutadiene (PB) or polyisoprene (PI) is one such example. Specifically, a recent study of Han et al.[7] shows that when a PB is hydrogenated, yielding poly(ethylene-*co*-1-butene) (PEB), and mixed with a polystyrene (PS), χ for the PS/PEB pair becomes greater (i.e., more repulsive) than that for the PS/PB pair. We hasten to point out that PB and PI have different microstructures (1,2-, 1,4-, and 3,4-addition), depending upon the type of solvent employed for polymerization. In a nonpolar solvent (e.g., cyclohexane) PI has high 1,4-addition, while in a polar solvent (e.g., tetrahydrofuran (THF)) PI has high vinyl content (1,2- and 3,4-addition). Also, the microstructures of PB can be controlled using different types of initiator for polymerization of butadiene. Halasa et al.[8] have shown that PB with very high vinyl content can be synthesized using organolithium as initiator modified with bis-heterocyclic ethane compounds.

Very recently, we synthesized three homogeneous low-molecular-weight polystyrene-*block*-polyisoprene (SI diblock) copolymers by anionic polymerization using THF as solvent and then hydroxylated the polyisoprene (PI) blocks via hydroboration and oxidation,[9−11] yielding hydroxylated SI diblock copolymers (SI-OH). We have found that ODT was induced by the hydroxylation of homogeneous SI diblock copolymer, and the resultant SI-OH diblock copolymers were semicrystalline, whereas the SI diblock copolymers employed for hydroxylation were amorphous. It should be mentioned that the molecular weights of the SI-OH diblock copolymers synthesized were increased by 3−9%, depending on the block length ratio of the corresponding SI diblock

10.1021/ma011089b CCC: $22.00
Published on Web 12/21/2001

copolymer, suggesting that the ODT observed in the SI-OH diblock copolymers cannot be explained by the increase in molecular weight. Cloud point measurements via light scattering of binary mixtures of PS and hydroxylated PI, PI-OH, have indicated strong repulsive segmental interactions between PS and PI-OH, the extent of which was found to increase with increasing degree of hydroxylation of PI. It is observed further via in-situ infrared spectroscopy that the strength of hydrogen bonding in SI-OH diblock copolymer decreases with increasing temperature. In this paper we report the origin of ODT observed in the SI-OH diblock copolymers that were obtained from hydroxylation of homogeneous SI diblock copolymer.

Experimental Section

Synthesis of SI Diblock Copolymers. THF was vacuum-distilled from sodium/benzophenone (deep purple color) into the reactor. 9-Borabicyclo[3.3.1]nonane (9-BBN, 0.5 M solution in THF) (Aldrich), pyridine (99.8% anhydrous), and *sec*-butyllithium (BuLi) (Aldrich, 1.3 M solution in cyclohexane) were used as received. Styrene (Fisher) was stirred with freshly ground calcium hydride (Aldrich, 95% purity) for 2 days at room temperature and distilled into a flask containing dibutylmagnesium (Aldrich, 1.0 M solution in heptane) after distilling the heptane out of the flask under high vacuum. Isoprene (Aldrich, 99% in purity) was dried over calcium hydride for 2 days, which was then distilled into a flask with dibutylmagnesium, stirred for 2 h prior to use, and the isoprene was distilled onto *n*-BuLi.

For the synthesis of SI diblock copolymers, the apparatus was dried rigorously under vacuum with heating. Just before polymerization, THF was distilled into a 500 mL flask, which was under vacuum and cooled at − 78 °C, and then styrene was distilled into the reactor under vacuum. Thirty minutes later, a predetermined amount of *sec*-BuLi was added into a reactor using a syringe. A red color soon developed. After polymerization of styrene, isoprene was distilled into the polymerization flask. The red color changed to yellow, and the polymerization continued for 4 h. To terminate the polymerization process, 1 mL of anhydrous degassed methanol was added into the reactor, making the solution look transparent. The solution was precipitated in methanol, filtered, washed with methanol, and dried at room temperature in a vacuum oven. Nuclear magnetic resonance (NMR) spectroscopy was used to determine the composition and microstructure of the block copolymers: SI diblock copolymer had 34% 1,2-addition, 59% 3,4-addition, and 7% 1,4-addition in PI block.

Hydroxylation of SI Diblock Copolymer. Hydroboration and oxidation of SI diblock copolymer were performed using the standard procedure,[9−11] following the route as schematically shown below. Briefly stated, an SI diblock copolymer was dissolved in THF and then precipitated in methanol, followed by drying under vacuum first at room temperature for 1 week and then at 40 °C for 1 day just before use. A predetermined amount of SI diblock was placed into a three-neck flask having a magnetic stirrer, and the flask was degassed by vacuum. THF was transferred into the three-neck flask by vacuum distillation and filled with argon gas.

The SI diblock copolymer in the flask was dissolved under agitation in THF. After a period, the system became a homogeneous solution at room temperature. The solution was then cooled to −15 °C, and 1.05 mol of 9-borabicyclo[3.3.1]-nonane (0.5 M 9-BBN solution) was added to the flask under argon gas using a syringe. The mixture was subsequently stirred for 24 h at room temperature, after which 1 mL of anhydrous methanol was injected into the flask, using a syringe, before the reaction solution was cooled to −25 °C. The mixture was stirred for 1 h to remove unreacted 9-BBN, and then 2 mol of sodium hydroxide (6 M aqueous solution) was transferred into the system at −25 °C. After 30 min, 3.2 mol of 30 wt % aqueous solution of hydrogen peroxide was added to the reactor very slowly; the solution was kept for 2 h. The

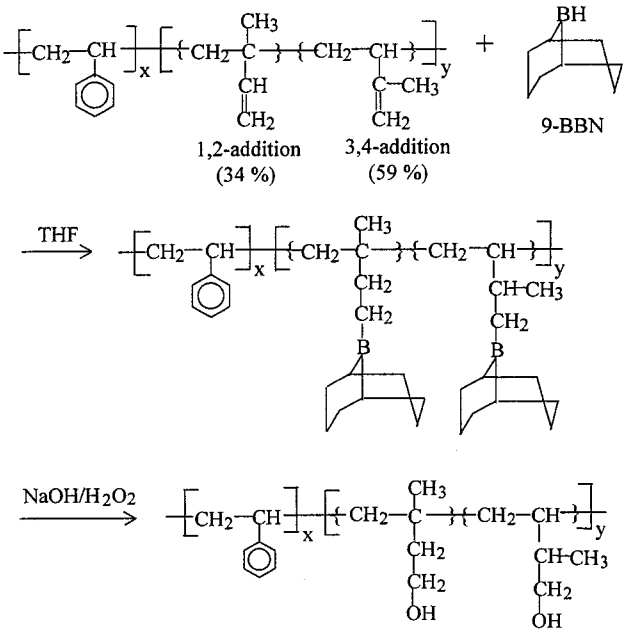

temperature of the solution was increased gradually to room temperature and stirred for 3 h, followed by slow heating to 40 °C, and held there for 2 h. Upon cooling to room temperature, the solution was poured into a mixture of distilled water and sodium chloride, from which a crude product, SI-OH, was precipitated out. The precipitate was washed three times with distilled water and filtered. The procedure described by Chung et al.[10] was adapted to remove the boric acid, $B(OH)_3$, which could be a potential source of cross-linking reaction later, in the precipitate. Namely, the crude product was put into methanol to form a suspension and distilled at 58−60 °C to remove $B(OH)_3$, until no further distillate could be collected. The distillation was repeated for 1.5 h (bp of CH_3OH = 65 °C; bp of $CH_3OH-B(OH)_3$ = 58 °C). Because $B(OH)_3$ is a byproduct of the oxidation, it was not effectively removed by washing with water. The best method for removing $B(OH)_3$ from the crude product was the distillation in the presence of CH_3OH at 58−60 °C. After distillation, the solid product was filtered and dried under vacuum for 3 days at 30 °C. To obtain different degrees of hydroxylation of the PI block in an SI diblock copolymer, the amount of reagent was controlled.[10] The degree of hydroxylation was determined using NMR and infrared (IR) spectroscopies.

Sample Preparation. Samples for rheological measurements and transmission electron microscopy (TEM) were prepared by solvent casting. Solvent casting was done by first dissolving a predetermined amount of polymer in toluene or THF in the presence of 0.1 wt % antioxidant (Irganox 1010, Ciba-Geigy Group) and then slowly evaporating the solvent at room temperature for 1 week in a fume hood. The cast sample with a thickness of about 1 mm was dried further in a vacuum oven at room temperature for 1 week and then at 10 °C above the glass transition temperature (T_g) for 3 days to completely remove the residual solvent. Samples for differential scanning calorimetry (DSC), NMR spectroscopy, and gel permeation chromatography (GPC) were used after drying in a vacuum oven.

Structure Characterization. The chemical structures of the polymers synthesized were characterized using NMR spectroscopy and Fourier transform infrared (FTIR) spectroscopy. For such purposes, both ^{13}C and ^{1}H NMR spectra were obtained using a spectrometer (Varian Gemini-200, 200 MHz). Films suitable for FTIR were prepared by casting 2% (w/v) solution in THF or chloroform directly on the KBr salt plate. Film thickness was adjusted, such that the maximum absorbance of any band was less than 1.0, at which the Beer−Lambert law is valid. It was slowly dried for 24 h in a fume hood until most of the solvent evaporated and then dried at 70 °C for a few days in a vacuum oven. Samples were then

Table 1. Molecular Characteristics of the SI and SI-OH Diblock Copolymers Synthesized in This Study

sample code	M_n (g/mol)[a]	M_n (g/mol)[b]	M_w/M_n[c]	PS (wt frac)[d]	morphology
SI-5/6	1.03×10^4 [a]	1.03×10^4 [b]	1.08	0.45	homogeneous
SI-10/6	1.51×10^4 [a]	1.52×10^4 [b]	1.09	0.65	homogeneous
SI-14/3	1.70×10^4 [a]	1.70×10^4 [b]	1.08	0.84	homogeneous
SI-5/6-OH	1.12×10^4 [e]	1.12×10^4 [e]	1.07	0.41	lamellae
SI-10/6-OH	1.64×10^4 [e]	1.64×10^4 [e]	1.09	0.60	lamellae
SI-14/3-OH	1.76×10^4 [e]	1.76×10^4 [e]	1.08	0.81	cylinders

[a] Determined from vapor pressure osmometry. [b] Determined from membrane osmometry. [c] Determined from GPC. [d] Determined from ^{1}H NMR spectroscopy. [e] Calculated from stoichiometry.

Table 2. Molecular Characteristics of the PI-OH Synthesized in This Study

sample code	M_n (g/mol)[a]	M_w/M_n[b]	deg of hydroxylation (%)[c]
PI-4	3600[a]	1.09	0
PI-OH-5	3600[d]	1.08	5
PI-OH-50	4000[d]	1.09	50
PI-OH-80	4500[d]	1.08	80
PI-OH-100	5000[d]	*e*	100

[a] Determined from vapor pressure osmometry. [b] Determined from GPC. [c] Determined from ^{1}H NMR spectroscopy. [d] Calculated from stoichiometry. [e] Unable to determine it owing to partial solubility in THF.

stored in a vacuum oven until use. FTIR spectra were obtained using a Perkin-Elmer spectrometer (model 16PC FTIR). Spectral resolution was maintained at 4 cm^{-1}. For in-situ FTIR measurement, the temperature was measured at the sample surface and controlled within ±1.0 °C using a proportional-integral-derivative controller. Specimens were maintained at a preset temperature for 5 min prior to data acquisition. Dry argon gas was used to purge the sample compartment in order to reduce the interference of water and carbon dioxide in the spectrum.

Molecular Weight Determination. The number-average molecular weight (M_n) of a low-molecular-weight PI and three SI diblock copolymers synthesized was determined using vapor pressure osmometry (Knauer) and also membrane osmometry (Jupiter Instrument), and the polydispersity (M_w/M_n) was determined using GPC (Waters). The results are summarized in Tables 1 and 2. Also given in Table 1 is the weight fraction of polystyrene in each SI diblock copolymer, which was determined using ^{1}H NMR spectroscopy.

Differential Scanning Calorimetry (DSC). Thermal transition temperatures of SI and SI-OH diblock copolymers were determined using DSC (Perkin-Elmer 7 series). All DSC runs were made under a nitrogen atmosphere with heating and cooling rates of 20 or 10 °C/min.

Polarizing Optical Microscopy. A hot-stage (TH-600 type, Linkham Scientific Co.) microscope (Nikon, model Optiphoto polXTP-11) with a camera, a programmable temperature controller, and photomicrographic attachment was used to take pictures, under cross-polarized light, of the film solvent cast on a slide glass.

Cloud Point Measurement. Cloud points of PS/(PI-OH) mixtures were measured on a thin film, which was prepared by dissolving predetermined amounts of PS and PI-OH in toluene or THF (ca. 10% solution). A few drops of this solution were placed on a slide glass and dried. The solvent was evaporated slowly at room temperature in a fume hood and then in a vacuum oven at an elevated temperature. The cloud point of a specimen was determined using laser light scattering. Specifically, a slide glass containing a sample was placed on the hot stage of the sample holder attached with a programmable temperature controller. A low-power He−Ne laser (wavelength of 635 nm) was used as the light source, and a photodiode was used as the detector. A sample was first heated to a temperature slightly (ca. 20 °C) above the cloud point (i.e., in the isotropic region) followed by a slow cooling into the two-phase region where a change in light intensity was noticeable, and then the specimen was heated again at a preset rate (0.5−5 °C/min), during which information on both temperature and the intensity of scattered light was stored on a diskette. For each composition, cloud point measurements were repeated three to five times until data were reproducible, and a fresh sample was used for each experimental run. Seven to nine compositions from 10/90 to 90/10 PS/(PO-OH) blend ratios were used to measure cloud point.

Transmission Electron Microscopy (TEM). TEM images of specimens were taken at room temperature. The ultrathin sectioning (50−70 nm) was performed by cryoultramicrotomy at −80 °C for SI diblock copolymers and at room temperature for SI-OH diblock copolymers. These temperatures, which are below the T_g of the respective block copolymers, were chosen to attain the rigidity of the specimen. This was done using a Reichert Ultracut E low-temperature sectioning system. A transmission electron microscope (JEM1200EX 11, JEOL) operated at 120 kV was used for taking images of the specimens stained with osmium tetroxide vapor for SI diblock copolymers and SI-OH diblock copolymers.

Oscillatory Shear Rheometry. An advanced Rheometric expansion system (ARES) (Rheometrics Scientific) was used in the oscillatory mode with a parallel-plate fixture (8 mm diameter). Dynamic frequency sweep experiments were conducted to measure the storage and loss moduli (G' and G'') as a function of angular frequency (ω) ranging from 0.03 to 100 rad/s at various temperatures. A fixed strain of 0.04 was used to ensure that measurements were taken well within the linear viscoelastic range of the materials investigated. The frequency sweep experiment at a preset temperature lasted for about 45 min, and the temperature control was accurate to within ±1 °C. Dynamic temperature sweep experiments under isochronal conditions were also conducted at $\omega = 0.01$ rad/s during heating, for which temperature was increased 2 °C/min stepwise. All measurements were conducted under a nitrogen atmosphere in order to avoid oxidative degradation of the samples.

Results and Discussion

Figure 1 gives ^{1}H NMR spectra for SI-5/6 and SI-5/6-OH. It can be seen in Figure 1 that there are no discernible amounts of 1,2- and 3,4-addition, and insignificant amounts of 1,4-addition are present in the SI-5/6-OH. This observation, together with the appearance of a spectrum at $\delta = 4.38$ ppm, representing the hydroxyl group, ensures us that hydroboration/oxidation reaction hydroxylation went nearly to completion. Similar observations, not presented here, were made for SI-10/6-OH and SI-14/3-OH. In the ^{1}H NMR spectra for PI block in $CDCl_3$, the chemical shifts are assigned as $[-CH_2-C\mathbf{H}{=}C(CH_3)-CH_2-]$ (1 proton) at $\delta = 5.01$ ppm, $[-CH_2-CH(C\mathbf{H}{=}CH_2)-]$ (1 proton) at $\delta = 5.71$ ppm, $[-CH_2-CH(CH{=}C\mathbf{H}_2)-]$ (2 protons) at $\delta = 4.86$ ppm, and $[-CH_2-CH(C(CH_3){=}C\mathbf{H}_2)-]$ (2 protons) at $\delta = 4.65$ ppm. In the ^{1}H NMR spectra for PI-OH block in DMSO, the chemical shifts are assigned as follows: $-O\mathbf{H}$ (1 proton) at $\delta = 4.38$ ppm and $-C\mathbf{H}_2-OH$ (2 protons) at $\delta = 3.36$ ppm.

Figure 2 gives FTIR spectra for SI-14/3-OH, SI-10/6-OH, and SI-5/6-OH. Also given in Figure 2, for comparison, are FTIR spectra for SI-5/6. It is seen that virtually all the double bonds (at 1640 and 910 cm^{-1})

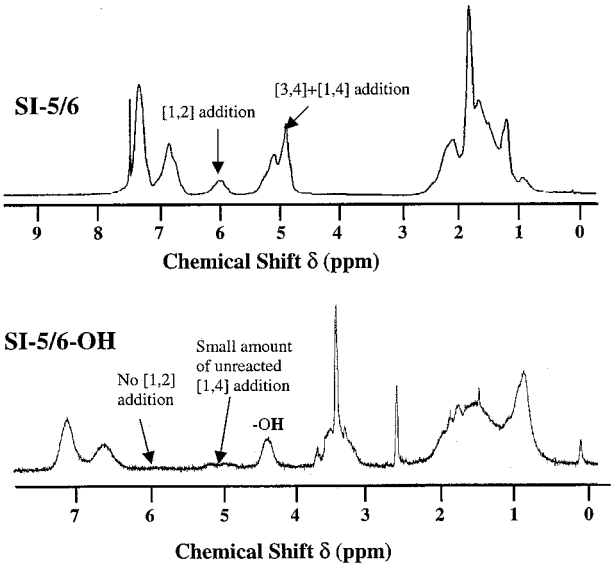

Figure 1. ^{1}H NMR spectra for SI-5/6 and SI-5/6-OH diblock copolymers.

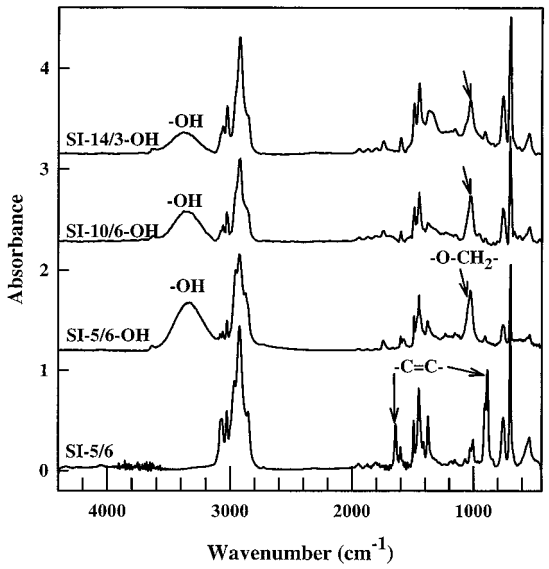

Figure 2. IR spectra for SI-14/3-OH, S1-10/6-OH, SI-5/6-OH, and SI-5/6 diblock copolymers at room temperature.

in the PI blocks of SI diblock copolymer have been hydroxylated, showing little (or no) double bonds in the SI-OH diblock copolymers. In SI-OH diblock copolymers, hydrogen-bonded and free hydroxyl group appears at 3330 and 3630 cm^{-1}, respectively. The hydrogen-bonded and free −OH groups will be elaborated on later. In the FTIR spectra for PI and PI-OH blocks, the absorption bands are assigned as −C═C− stretching at 910 and 1640 cm^{-1}, O−H stretching at 3340 cm^{-1}, and −O−CH_2 stretching at 1055 cm^{-1}.

The GPC traces of the three SI diblock copolymers and three SI-OH diblock copolymers are given in Figure 3, showing that *no* side reactions occurred during the hydroxylation of SI diblock copolymer, because the breadth of GPC trace is not altered after the hydroxylation of SI diblock copolymer. The GPC traces in Figure 3 give an impression that the molecular weight of the SI-OH diblock copolymer is slightly lower than that of the corresponding SI diblock copolymer, provided that the hydrodynamic volume of the SI-OH diblock copolymer molecules is the same as that of SI diblock

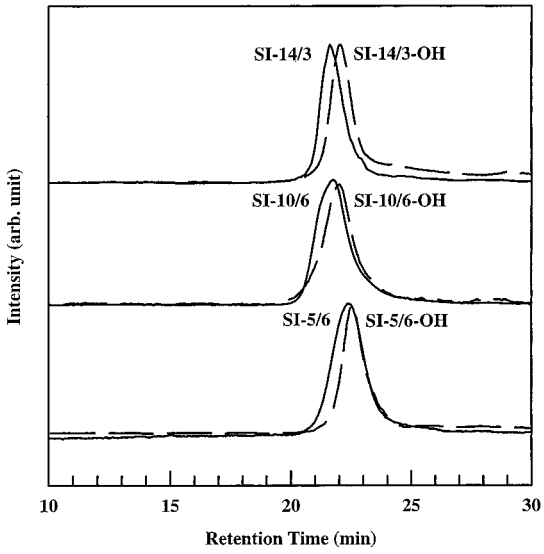

Figure 3. GPC traces of SI-5/6, SI-5/6-OH, S1-10/6, S1-10/6-OH, SI-14/3, and SI-14/3-OH diblock copolymers.

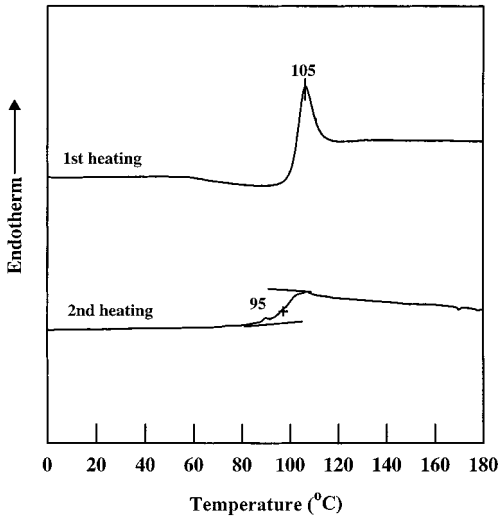

Figure 4. DSC traces of SI-5/6-OH diblock copolymer in the first and second heating cycles.

copolymer molecules. In view of the fact that the SI-OH diblock copolymer forms hydrogen bonding, as will be elaborated on below, it is reasonable to speculate that the SI-OH diblock copolymer would have a smaller hydrodynamic volume. This means that accurate determinations of the molecular weight of the SI-OH diblock copolymer from a GPC trace is not possible unless information on the hydrodynamic volume is available. In the absence of information on the hydrodynamic volume of SI-OH diblock copolymer molecules, in this study we have estimated the molecular weight of the three SI-OH diblock copolymers synthesized using information on the degree of hydroxylation, and they are summarized in Table 1. It is seen that the molecular weights of the SI-OH diblock copolymers are 3−9% higher, depending on the block length ratio, than the corresponding SI copolymers.

Thermal Transition and Crystallinity in SI-OH Diblock Copolymer. Figure 4 gives DSC traces for an as-cast SI-5/6-OH specimen in the first and second heating cycles. It is seen that during the first cycle the as-cast SI-5/6-OH specimen has an endothermic peak, representing the melting temperature, at ca. 105 °C, but during the second heating cycle no endothermic peak

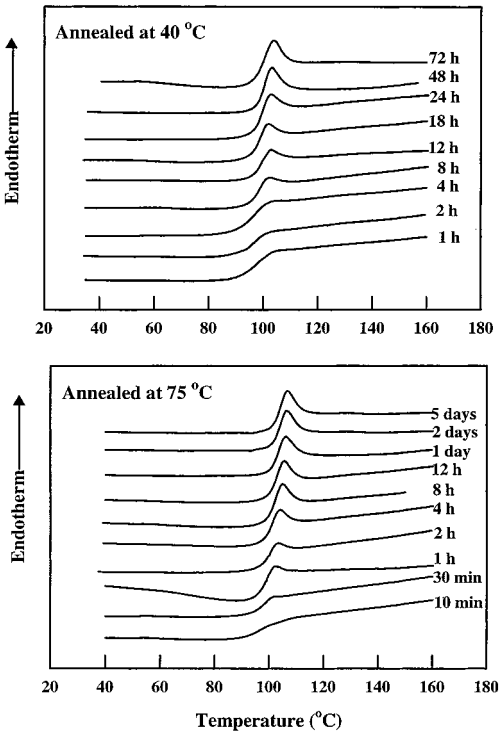

Figure 5. DSC traces of SI-5/6-OH diblock copolymer annealed at 40 and 75 °C for varying periods as indicated.

is discernible. This observation suggested to us that the rate of crystallization in SI-5/6-OH was very slow. Therefore, we investigated the effect of annealing conditions on the rate of crystallization in SI-5/6-OH. The upper panel of Figure 5 gives DSC traces for SI-5/6-OH specimens that were annealed at 40 °C for varying periods ranging from 1 to 72 h, and the lower panel of Figure 5 gives DSC traces for SI-5/6-OH specimens that were annealed at 75 °C for varying periods ranging from 10 min to 5 days. In Figure 5 we observe that an endothermic peak begins to appear when a specimen was annealed for 8 h at 40 °C and that an endothermic peak begins to appear when a specimen was annealed for 1 h at 75 °C. This observation indicates that the rate of crystallization in SI-5/6-OH was accelerated as the annealing temperature was increased from 40 to 75 °C. Figure 6 describes the effect of annealing time on the heat of fusion, ΔH_f, for SI-5/6-OH at two different annealing temperatures, 40 and 75 °C. In Figure 6 we observe that ΔH_f has not attained an equilibrium value even after annealing for 72 h at 40 °C, while ΔH_f has attained an equilibrium value after annealing for 50 h at 75 °C. The observations made in Figure 6 clearly indicate that the rate of crystallization in SI-5/6-OH is extremely slow. Notice further in Figure 6 that the values of ΔH_f for SI-5/6-OH are very small, compared to those for other semicrystalline polymers (e.g., nylon, polypropylene), suggesting that the degree of crystallinity in SI-5/6-OH is very low.

Figure 7 gives a POM image of an as-cast SI-5/6-OH and PI-13-OH specimen that were taken at room temperature. The micrographs were taken using a specimen that had been cast from THF/H_2O (95:5 v/v) mixed solvent and dried at 70 °C for 1 day in a vacuum oven. It is clearly seen that both SI-5/6-OH and PI-13-OH have spherulites of crystalline phase.

There can be more than one reason why SI-OH diblock copolymers undergo very slow crystallization

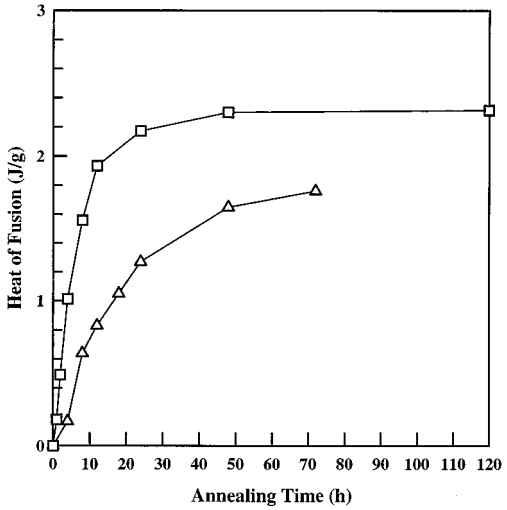

Figure 6. Plots of heat fusionfor SI-5/6-OH diblock copolymer vs annealing time under isothermal conditions at 40 (△) and 75 °C (□).

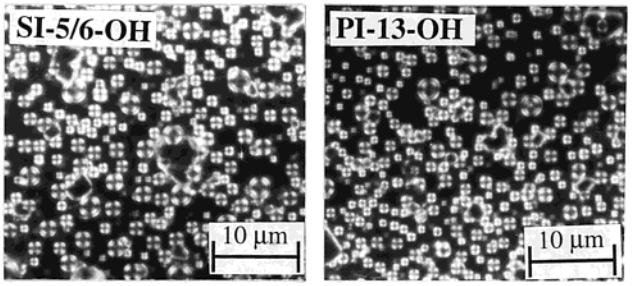

Figure 7. POM image, taken at room temperature, of SI-5/6-OH and PI-13-OH showing spherulites.

and have such small values of ΔH_f (ca. 2.5 J/g), compared to that of such semicrystalline polymers, as nylon and polypropylene, which undergo fast crystallization and have much larger values of ΔH_f (e.g., ΔH_f = ca. 60 J/g for nylon 6; ΔH_f = ca. 216 J/g for polypropylene). One prevailing reason appears to be the steric hindrance of the PS block in the main chain of the SI-OH diblock copolymer, while hydroxyl groups are attached to the PI block. That is, even after the hydroxylation of the PI block, the main chain of the SI-OH diblock copolymer might still have the tendency to be randomly distributed while the hydroxyl groups attached to the PI block tend to have an ordered structure owing to hydrogen bonding.

Order−Disorder Transition in SI-OH Diblock Copolymers. In the past, oscillatory shear rheometry has extensively been used to investigate ODT in block copolymer.[12] The results of dynamic frequency sweep experiment at various temperatures (plot of log G' vs log G''), and the results of isochronal dynamic temperature sweep experiment at an angular frequency ω = 0.01 rad/s (plot of log G' vs temperature) are given in Figure 8 for SI-10/6, in Figure 9 for SI-5/6, and in Figure 10 for SI-14/3. It should be mentioned that the log G' vs log G'' plot, which Neumann et al.[13] referred to as the Han plot, was obtained during heating with a predetermined temperature interval. A plot of log G' vs temperature was also obtained during heating using a step increase in temperature of 3 °C. This mode of dynamic temperature sweep experiment was different from the mode that increases the temperature continuously (a ramp mode). It is seen in Figures 8−10 that all three SI diblock copolymers follow the behavior of

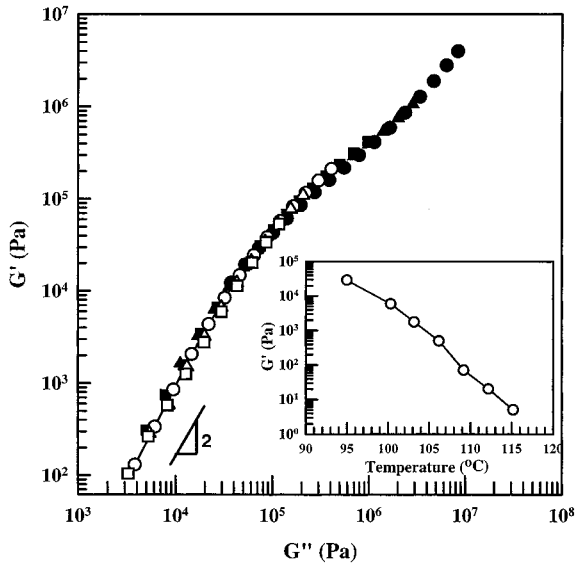

Figure 8. Han plots for SI-10/6 diblock copolymer at various temperatures: (●) 95, (▲) 100, (■) 105, (○) 110, (△) 115, and (□) 120 °C. The inset describes variations of G' with temperature during isochronal dynamic temperature sweep experiments of SI-10/6 diblock copolymer at $\omega = 0.01$ rad/s.

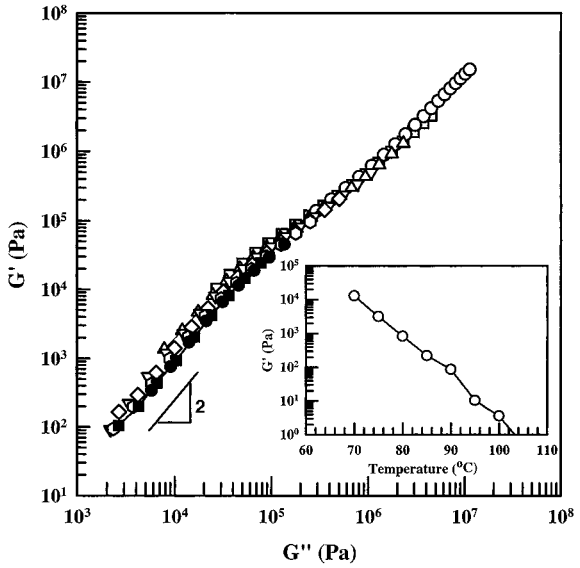

Figure 9. Han plots for SI-5/6 diblock copolymer at various temperatures: (○) 60, (□) 70, (△) 75, (▽) 80, (◇) 85, (⬠) 90, (●) 95, and (■) 100 °C. The inset describes variations of G' with temperature during isochronal dynamic temperature sweep experiments of SI-5/6 diblock copolymer at $\omega = 0.01$ rad/s.

homopolymers in that the Han plot in the terminal region has a slope of 2 and is independent of temperature over the entire range of temperatures tested, and the values of G' decrease monotonically with increasing temperature during the isochronal dynamic temperature sweep experiment. Earlier, such rheological behavior of homopolymers and random copolymers has been reported.[14,15] Thus, it is concluded that all three SI diblock copolymers (SI-10/6, SI-5/6, and SI-14/3) have no microdomains. Independent TEM study has confirmed the conclusion.

The results of the dynamic frequency sweep experiment at various temperatures and the results of the isochronal dynamic temperature sweep experiment at an angular $\omega = 0.01$ rad/s are given in Figure 11 for SI-10/6-OH, in Figure 12 for SI-5/6-OH, and in Figure

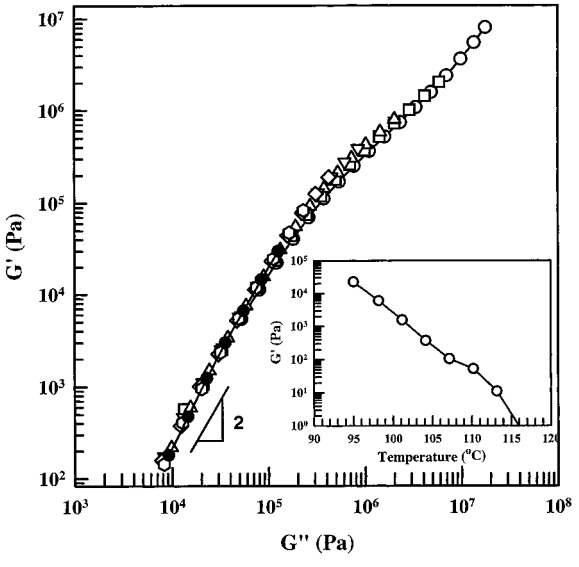

Figure 10. Han plots for SI-14/3 diblock copolymer at various temperatures: (○) 95, (□) 100, (△) 105, (▽) 110, (◇) 115, (⬠) 120, and (●) 125 °C. The inset describes variations of G' with temperature during isochronal dynamic temperature sweep experiments of SI-14/3 diblock copolymer at $\omega = 0.01$ rad/s.

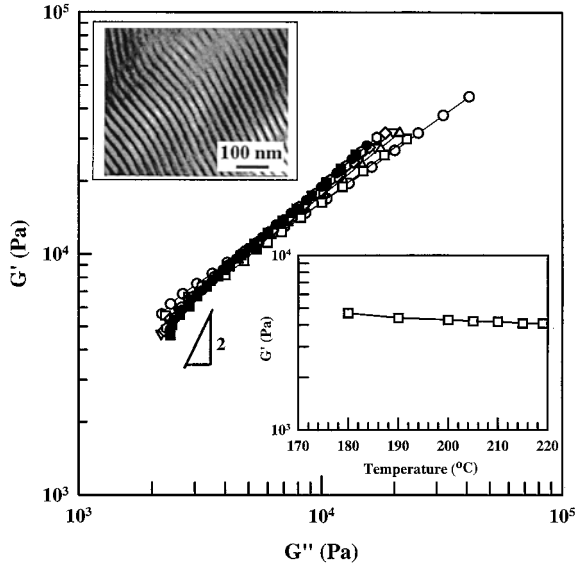

Figure 11. Han plots for SI-10/6-OH diblock copolymer at various temperatures: (○) 170, (□) 180, (△) 190, (▽) 195, (◇) 200, (⬠) 205, (●) 210, and (■) 215 °C. The inset describes variations of G' with temperature during isochronal dynamic temperature sweep experiments of SI-10/6-OH diblock copolymer at $\omega = 0.01$ rad/s.

13 for SI-14/3-OH. The following observations are worth noting in Figures 11−13. Referring to Figure 11, during the isochronal dynamic temperature sweep experiment the values of G' for SI-10/6-OH stay more or less constant over the entire range of temperatures tested (180−220 °C), indicating that no softening occurred in this block copolymer with increasing temperature. This rheological behavior is quite different from that of the corresponding SI diblock copolymer, SI-10/6 (see Figure 8). According to the rheological criterion applied to the isochronal dynamic temperature sweep experiment,[16] it can be concluded that SI-10/6-OH has T_{ODT} much higher than 220 °C. The Han plot given in Figure 11 reinforces the conclusion in that the Han plot in the terminal region has a slope less than 2 and exhibits a tempera-

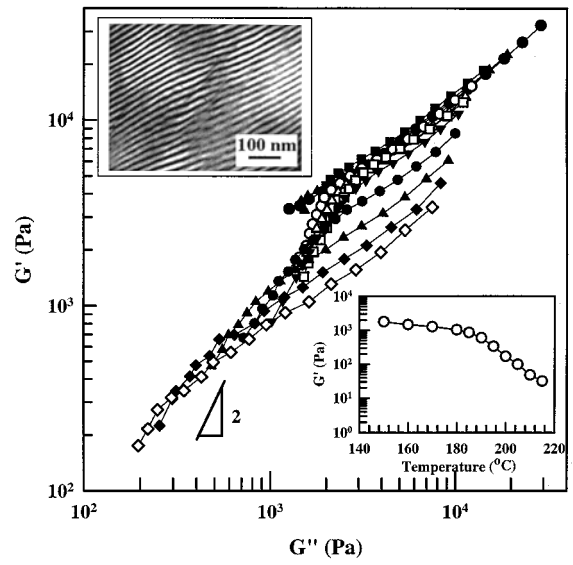

Figure 12. Han plots for SI-5/6-OH diblock copolymer at various temperatures: (○) 140, (□) 150, (△) 160, (▽) 170, (◇) 180, (⬡) 185, (●) 190, (■) 195, (▲) 200, (▼) 205, and (◆) 210 °C. The inset describes variations of G' with temperature during isochronal dynamic temperature sweep experiments of SI-5/6-OH diblock copolymer at $\omega = 0.01$ rad/s.

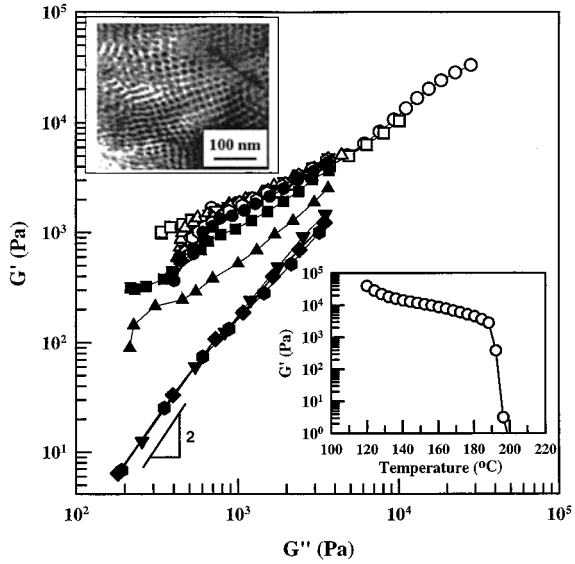

Figure 13. Han plots for SI-14/3-OH diblock copolymer at various temperatures: (○) 130, (□) 150, (△) 170, (▽) 180, (◇) 183, (⬡) 186, (●) 189, (■) 192, (▲) 195, (▼) 198, (◆) 200, and (⬢) 205 °C. The inset describes variations of G' with temperature during isochronal dynamic temperature sweep experiments of SI-14/3-OH diblock copolymer at $\omega = 0.01$ rad/s.

ture dependence. TEM study shows that SI-10/6-OH has lamellar microdomains, as shown in the inset of Figure 11. The readers are reminded that SI-10/6 has a 0.65 weight fraction of PS block and SI-10/6-OH has a 0.62 weight fraction of PS block (see Table 1); i.e., the block composition has changed only slightly after the SI-10/6 is hydroxylated. Note that the molecular weight of SI-10/6-OH is only ca. 9% higher than that of SI-10/6. Therefore, the lamellar microdomain structure in SI-10/6-OH that was induced by the hydroxylation of the homogeneous SI-10/6 cannot be explained by an argument of the increase in molecular weight by 9%. Below we will offer an explanation on the origin of the ODT observed in SI-10/6-OH.

Referring to Figure 12, during the isochronal dynamic temperature sweep experiment the values of G' for SI-5/6-OH stay more or less constant at temperatures up to 180 °C and then begin to decrease gradually with increasing temperature further to ca. 210 °C, the highest experimental temperature employed. That is, *no* particular temperature is discernible at which the value of G' drops precipitously, leading us to conclude that SI-5/6-OH has T_{ODT} higher than ca. 210 °C. Again, the temperature dependence of G' during isochronal dynamic temperature sweep experiment of SI-5/6-OH is quite different from that of the corresponding SI diblock copolymer, SI-5/6 (compare Figure 12 with Figure 9), suggesting that SI-5/6-OH has microdomains. Indeed, TEM study, as shown in the inset of Figure 12, reveals that SI-5/6-OH has lamellar microdomains. Note that the block composition has changed only slightly after SI-5/6 is hydroxylated, and the molecular weight of SI-5/6-OH is only ca. 9% higher than that of SI-5/6 (see Table 1). In Figure 12 we observe that the slope of the Han plot in the terminal region varies with temperature over the entire range of temperatures tested (140−210 °C), leading us to conclude that the T_{ODT} of SI-5/6-OH is higher than 210 °C, the highest experimental temperature.

Referring to Figure 13, during the isochronal dynamic temperature sweep experiment the values of G' for SI-14/3-OH begins to drop precipitously at ca. 190 °C, showing negligibly small values of G' at about 195 °C. According to the rheological criterion applied to the isochronal dynamic temperature sweep experiment,[16] it can be concluded that the T_{ODT} of SI-14/3-OH is about 195 °C. It is seen in Figure 13 that the Han plot begins to be independent of temperature at 195 °C, and its slope in the terminal region is 2 at $T \geq 195$ °C. Earlier, such a rheological criterion has been used for lamella- or cylinder-forming block copolymers.[17] TEM study, shown in the inset of Figure 13, reveals that SI-14/3-OH has hexagonally packed cylindrical microdomains. Again, the block composition has changed only slightly after SI-14/3 is hydroxylated, and the molecular weight of SI-14/3-OH is only ca. 3% higher than that of SI-14/3.

Phase Behavior of Binary Mixtures of PS and PI-OH. In this study we synthesized a PS having $M_n =$ 4100 g/mol and a PI having $M_n = 3600$ g/mol and then hydroxylated the PI, yielding PI-OH, with varying degrees of hydroxylation ranging from 5 to 100% as determined by ^{1}H NMR spectroscopy. It should be mentioned that the M_n of PS was determined against polystyrene standards using GPC, and the M_n of PI was determined using both vapor pressure osmometry and membrane osmometry. We prepared, via solution casting in toluene, binary mixtures of PS and PI-OH with varying compositions and determined, via light scattering, cloud points of each mixture following the procedures described in the Experimental Section. Figure 14 gives binodal curves determined from the cloud point measurements for PS/PI, PS/(PI-OH-5), PS/(PI-OH-50), PS/(PI-OH-80), and PS/(PI-OH-100) mixtures, where the numbers 5, 50, 80, and 100 refer to the percentage of hydroxylation. It is seen in Figure 14 that the binodal curve is shifted upward with increasing degree of hydroxylation of PI, indicating that repulsive segmental interactions between PS and PI-OH are increased with increasing degree of hydroxylation. This observation now explains that the ODT observed in the SI-10/6-OH,

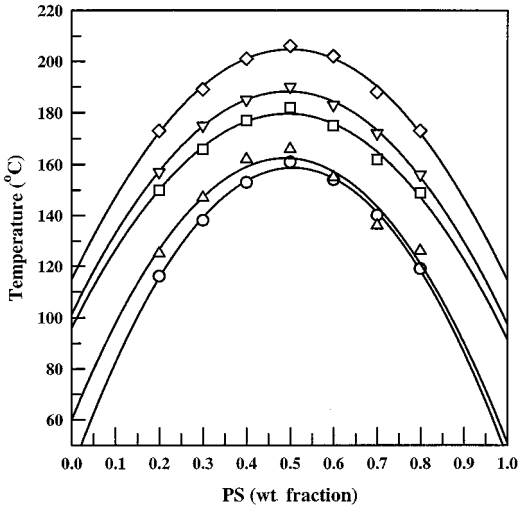

Figure 14. Binodal curves for (○) PS/PI binary mixtures, (△) PS/(PI-OH-5) binary mixtures, (□) PS/(PI-OH-50) mixtures, (▽) PS/(PI-OH-80) mixtures, and (◇) PS/(PI-OH-100) mixtures.

SI-5/6-OH, and SI-14/3-OH diblock copolymers (see Figures 11−13) is due to the large increase in the repulsive segmental interactions between the PS and PI-OH blocks in the respective block copolymers after the homogeneous SI diblock copolymers (SI-10/6, SI-5/6, and SI-14/3) were hydroxylated. It should be mentioned that, after 100% hydroxylation of PI block in the SI-10/6, SI-5/6, and SI-14/3 diblock copolymers, the molecular weight is increased only by 3−9%. Thus, such a small increase in molecular weight cannot possibly explain the very large upward shift in the binodal curves shown in Figure 14.

We wish to mention that, in the absence of specific interactions between components in a binary blend, binodal curves may be used to determine segmental interaction parameter with the aid of the Flory−Huggins theory. However, as presented above (see Figure 2) hydrogen bonding exists in the SI-OH diblock copolymer owing to the hydroxyl groups in the PI block (thus between PS and PI-OH in the binary mixtures). Under such circumstances the Flory−Huggins theory is not adequate to determine segmental interaction parameter. Further discussion of this subject is beyond the scope of this study.

Hydrogen Bonding in PI-OH and SI-OH Diblock Copolymers. In an effort to search for a physical origin in the strong tendency of phase separation in PS/(PI-OH) mixtures, shown in Figure 14, we have conducted in-situ FTIR experiment at various temperatures following procedures described in the Experimental Section.

Figure 15a gives FTIR spectra for neat PI and PI-OHs having varying degrees of hydroxylation ranging from 5 to 100%. It should be mentioned that partially hydroxylated PI-OHs are actually statistical copolymers. It is seen in Figure 15a that the area under the absorption band at 3330 cm^{-1} increases with increasing degree of hydroxylation, indicating the strength of the hydrogen-bonding interactions increases as the degree of hydroxylation of PI increases. This observation is clearly seen in Figure 15b, showing that the ratio A/A_{100} increases almost linearly with increasing degree of hydroxylation, where A_{100} denotes the area under the absorption band at 3330 cm^{-1} for 100% hydroxylated PI-OH.

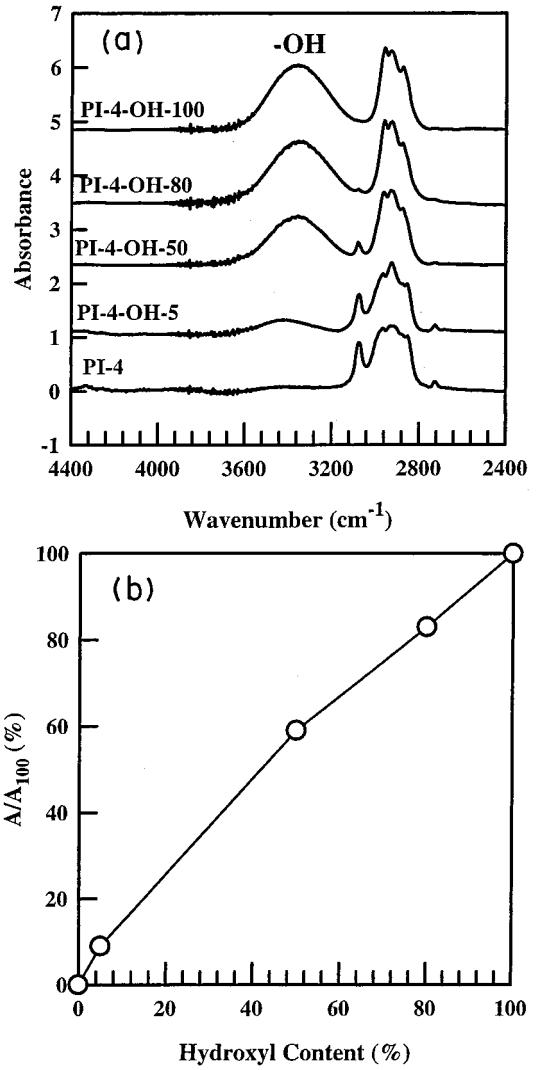

Figure 15. (a) FTIR spectra for neat PI and PI-OH having varying degrees of hydroxylation and (b) variations of the ratio A/A_{100} with degree of hydroxylation in PI-4, where A_{100} denotes the area under the absorption band at 3330 cm^{-1} for 100% hydroxylated PI-4.

Figure 16 gives FTIR spectra of the three SI-OH diblock copolymers, SI-5/6-OH, SI-10/6-OH, and SI-14/3-OH, at various temperatures ranging from 30 to 220 °C, where the absorption band at about 3330 cm^{-1} represents the stretching of −OH group. The following observations are worth noting in Figure 16. (i) At 30 °C most of the hydroxyl groups are hydrogen-bonded, as shown by the large peak at ca. 3330 cm^{-1} with a very small shoulder at 3440 cm^{-1}.[18,19] (ii) The temperature dependence of absorption bands at about 3330 cm^{-1} becomes weaker as the temperature is increased, indicating that the strength of hydrogen bonding is weakened with increasing temperature. (iii) The area under the absorption band at about 3330 cm^{-1} is largest for SI-5/6-OH, becoming smaller for SI-10/6-OH and much smaller for SI-14/3-OH. The decreasing trend of the area under the absorption band at 3330 cm^{-1} is due to the decrease in the percentage of −OH groups in each SI−OH diblock copolymer in the following descending order: SI-5/6-OH > SI-10/6-OH > SI-14/3-OH. It is interesting to observe in Figure 16 that the absorption peak of −OH groups in SI-5/6-OH and SI-10/6-OH still persists up to 220 °C, whereas almost all −OH groups in SI-14/3-OH disappears at ca. 200 °C.

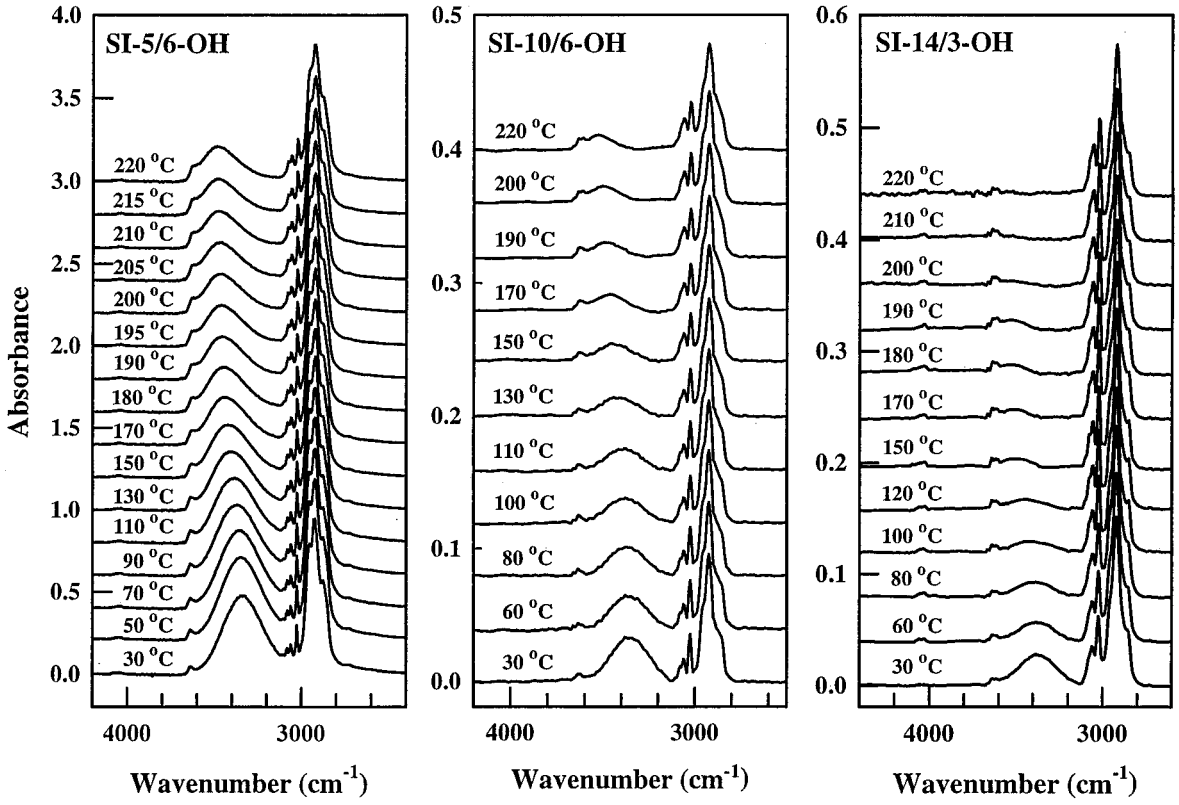

Figure 16. In-situ FTIR spectra at varying temperatures for SI-5/6-OH, SI-10/6-OH, and SI-14/3-OH diblock copolymers.

The broad −OH stretching peak is attributable to several different aggregation types of hydrogen bonding.[18,19] The hydrogen bonding at low-energy level disappears first as the temperature is increased. However, without the knowledge of temperature dependence of absorptivity coefficient, it is very difficult to conclude whether or not the concentration of free −OH group is increased as the temperature is increased. Note that absorptivity coefficient represents an average value of the strengths of functional groups. The areas under the absorption band at 3330 cm^{-1} (i.e., hydrogen-bonded −OH group) at temperatures T and 30 °C; A and A_0 are calculated using a curve-fitting procedure.[20] The variation of the ratio $A(T)/A_0$ with temperature is given in Figure 17, showing that the ratio $A(T)/A_0$ decreases with increasing temperature in all three SI-OH diblock copolymers. The following observations are worth noting in Figure 17. The amount of hydrogen-bonded −OH group in SI-5/6-OH decreases steadily with increasing temperature, and yet about 40% of hydrogen-bonded −OH groups still persist at 220 °C. The amount of hydrogen-bonded −OH group in SI-10/6-OH decreases rapidly with increasing temperature until reaching ca. 135 °C, at which about 22% of hydrogen-bonded −OH groups still persist, and then the remaining hydrogen-bonded −OH groups decrease at much a slower rate as the temperature is increased further to 220 °C. The amount of hydrogen-bonded −OH group in SI-14/3-OH decreases rapidly with increasing temperature until reaching ca. 130 °C, at which about 18% of hydrogen-bonded −OH groups persist, and then the remaining hydrogen-bonded −OH groups virtually disappear as the temperature is increased further to 200 °C.

Figure 17 can now be used to explain why, among the three SI-OH diblock copolymers synthesized in this study, SI-14/3-OH has the lowest T_{ODT} (see Figure 13) while SI-10/6-OH has the highest T_{ODT} (see Figure 11).

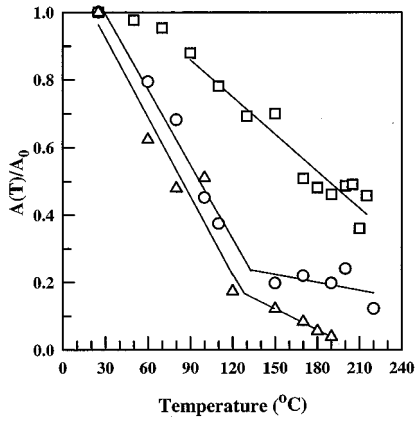

Figure 17. Variations of the ratio $A(T)/A_0$ for the O−H stretching absorption bands in the FTIR spectra with temperature for SI-5/6-OH (○), SI-10/6-OH (△), and SI-14/3-OH (□), where $A(T)$ represents the areas under the O−H stretching absorption bands at temperature T and A_0 is the areas under the O−H stretching absorption bands at 30 °C.

Note that, among the three SI-OH diblock copolymers, SI-14/3-OH has the smallest amount of PI-OH block and hence the least amount of hydrogen bonding. This is reflected in Figure 17, showing that virtually no hydrogen bonding remains at ca. 200 °C, which is very close to the T_{ODT} of SI-14/3-OH determined from oscillatory shear flow experiment (see Figure 13). It can then be concluded that the disappearance of hydrogen bonding in SI-14/3-OH at ca. 200 °C is responsible for the ODT observed in the block copolymer. Note that SI-10/6-OH has twice as many PI-OH blocks compared to SI-14/3-OH, although SI-10/6-OH has the molecular weight slightly lower (ca. 11%) than SI-14/3-OH. Referring to Figure 17, about 20% of hydrogen bonding in SI-10/6-OH still persists at 200 °C, and the hydrogen bonding decreases extremely slowly with increasing temperature

further. It can thus be concluded that the seemingly very high T_{ODT} (>220 °C) of SI-10/6-OH (see Figure 11) is attributable to the presence of hydrogen bonding at temperature as high as 240 °C (see Figure 17). On the other hand, SI-5/6-OH still has ca. 40% hydrogen bonding at 210 °C (see Figure 17), and its T_{ODT} is higher than 210 °C (see Figure 12). Thus, there is a correlation between T_{ODT} and the presence of hydrogen bonding in SI-5/6-OH, consistent with the observations made above for SI-10/6-OH.

Concluding Remarks

In this study we have shown that hydroxylation of homogeneous SI diblock copolymer induced the formation of microdomain structure in the SI-OH diblock copolymer, and the T_{ODT} of an SI-OH diblock copolymer increased dramatically with a slight increase in the amount of PI-OH block, while the molecular weight is increased only slightly (3−9%) after the hydroxylation of an SI diblock copolymer. Since it is well-known that the T_{ODT} of the block copolymer is increased as the extent of repulsive segmental interactions between the constituent blocks is increased, using cloud point measurement we have investigated the phase behavior of binary blends of PS and PI-OH. We found that PS/(PI-OH) binary blends exhibit upper critical solution temperature (UCST), and the binodal curve is shifted upward (i.e., the blends become increasingly immiscible) as the degree of hydroxylation of PI is increased. That is, segmental interactions between PS and PI-OH become strongly repulsive as the degree of hydroxylation of PI is increased. Thus, we can conclude that the formation of microdomains observed in the SI-OH diblock copolymers, which were obtained by the hydroxylation of homogeneous SI diblock copolymers, is attributable to the presence of strong repulsive interactions between PS and PI-OH blocks.

We then investigated the origin of the strong repulsive interactions between PS and PI-OH blocks in SI-OH diblock copolymers. Using in-situ FTIR spectroscopy, we found that the SI-OH diblock copolymer forms hydrogen bonding, the strength of which decreases with increasing temperature. Thus, we conclude that the strong repulsive interactions observed between PS and PI-OH blocks in SI-OH diblock copolymers have originated from the intra- or intermolecular hydrogen bonding among the PI-OH blocks. This is quite different from the situation where repulsive segmental interactions are increased when PB blocks in a polystyrene-*block*-polybutadiene (SB diblock) copolymer are hydrogenated, yielding polystyrene-*block*-poly(ethylene-*co*-1-butene) (SEB diblock) copolymer, because *no* hydrogen bonding is formed in the PEB blocks of the SEB diblock copolymer. That is, there are no specific interactions between PS and PEB blocks in the SEB diblock copolymer.

We also found that the SI-OH diblock copolymer is crystalline as determined from DSC and POM, while the corresponding SI diblock copolymer is glassy. We believe that the crystallinity of the SI-OH diblock copolymer has originated from the presence of hydrogen bonding. However, we found that, compared to other semicrystalline polymers, the degree of crystallinity in the SI-OH diblock copolymer is very weak and the rate of crystallization, upon cooling, is extremely slow. This is attributable to the steric hindrance of the PS blocks in the main chain of the SI-OH diblock copolymer, where the hydroxyl groups attached onto the PI blocks tend to form an ordered structure owing to hydrogen bonding. The slow rate of crystallization in the SI-OH diblock copolymer is attributable, owing to the steric hindrance of PS blocks in the main chain, to the slow rearrangement of hydrogen bonding among the hydroxyl groups in PI-OH blocks.

Finally, we conclude that the formation of microdomains observed in the SI-OH diblock copolymers, which were obtained by the hydroxylation of homogeneous SI diblock copolymers, is attributable to the presence of hydrogen bonding among the hydroxyl groups in PI-OH blocks.

References and Notes

(1) Hashimoto, T. In *Thermoplastic Elastomers*; Legge, N. R., Holden, G., Schroeder, H. E., Eds.; Hanser: Munich, 1987; Chapter 12, Section 3. Second Edition: Holden, G., Legge, N. R., Quirk, R., Schroeder, H. E., Eds.; 1996; Chapter 15A.
(2) Bates, F. S.; Fredrickson, G. H. *Annu. Rev. Phys. Chem.* **1990**, *41*, 525.
(3) Helfand, E.; Wasserman, Z. R. In *Developments in Block Copolymers*; Goodman, I., Ed.; Applied Science: New York, 1982; Chapter 4.
(4) Leibler, L. *Macromolecules* **1980**, *13*, 1602.
(5) Vavasour, J. D.; Whitmore, M. D. *Macromolecules* **1992**, *25*, 5477.
(6) Matsen, M. W.; Schick, M. *Phys. Rev. Lett.* **1994**, *72*, 2660.
(7) Han, C. D.; Chun, S. B.; Hahn, F. S.; Harper, S. Q.; Savickas, P. J.; Meunier, D. J.; Li, L.; Yalcin, T. *Macromolecules* **1998**, *31*, 394.
(8) Halasa, A.; Lohr, D. F.; Hall, J. E. *J. Polym. Sci., Polym. Chem. Ed.* **1981**, *19*, 1357.
(9) Brown, H. C. *Hydroboration*; Benjamin: New York, 1962.
(10) Chung, T. C.; Raate, M.; Berluche, E.; Schulz, D. N. *Macromolecules* **1988**, *21*, 1903.
(11) Mao, G.; Wang, J.; Clingman, S. C.; Ober, C. K.; Chen, J. T.; Thomas, E. L. *Macromolecules* **1997**, *30*, 2556.
(12) Han, C. D.; Baek, D. M.; Kim, J. K.; Ogawa, T.; Sakamoto, N.; Hashimoto, T. *Macromolecules* **1995**, *28*, 5043 and references therein.
(13) Neumann, C.; Loveday, D. R,; Abetz, V.; Stadler, R. *Macromolecules* **1998**, *31*, 2493. These authors referred to the logarithmic plot of G' vs G'' as the Han plot.
(14) Han, C. D.; Jhon, M. S. *J. Appl. Polym. Sci.* **1986**, *32*, 3809.
(15) Han, C. D. *J. Appl. Polym. Sci.* **1988**, *35*, 167.
(16) (a) Gouinlock, E. V.; Porter, R. S. *Polym. Eng. Sci.* **1977**, *17*, 535. (b) Chung, C. I.; Lin, M. I. *J. Polym. Sci., Polym. Phys. Ed.* **1978**, *16*, 545. (c) Widmaier, J. M.; Meyer, G. C. *J. Polym. Sci., Polym. Phys. Ed.* **1980**, *18*, 2217.
(17) (a) Han, C. D.; Kim, J. *J. Polym. Sci., Polym. Phys. Ed.* **1987**, *25*, 1741. (b) Han, C. D.; Kim, J.; Kim, J. K. *Macromolecules* **1989**, *22*, 383. (c) Han, C. D.; Baek, D. M.; Kim, J. K. *Macromolecules* **1990**, *23*, 561.
(18) Vinogradov, S. N.; Linnell, R. H. In *Hydrogen Bonding*; van Nostrand Reinhold: New York, 1971; Chapter 5.
(19) Josten, D. M.; Schaad, L. In *Hydrogen Bonding*; Marcel Dekker: New York, 1974; Chapters 1 and 2.
(20) (a) Yoon, P. J. Effect of Thermal History on the Rheology of Thermoplastic Polyurethanes. Doctoral Dissertation, University of Akron, Akron, OH, 1999. (b) Yoon, P. J.; Han, C. D. *Macromolecules* **2000**, *33*, 2171.

MA011089B